Neuron, Vol. 22, 707–717, April, 1999, Copyright ©1999 by Cell Press

Retinal Axon Target Selection in *Drosophila* Is Regulated by a Receptor Protein Tyrosine Phosphatase

Paul A. Garrity,*†# Chi-Hon Lee,*# Iris Salecker,*# Heather C. Robertson,† Chand J. Desai,‡ Kai Zinn,§ and S. Lawrence Zipursky*‖
*Howard Hughes Medical Institute
Department of Biological Chemistry
Molecular Biology Institute
University of California School of Medicine
Los Angeles, California 90095
†Department of Biology
Massachusetts Institute of Technology
Cambridge, Massachusetts 02138
‡Center for Molecular Neuroscience
Vanderbilt University Medical Center
Nashville, Tennessee 37232
§Division of Biology
California Institute of Technology
Pasadena, California 91125

Summary

Different *Drosophila* photoreceptors (R cells) connect to neurons in different optic lobe layers. R1–R6 axons project to the lamina; R7 and R8 axons project to separate layers of the medulla. We show a receptor tyrosine phosphatase, PTP69D, is required for lamina target specificity. In *Ptp69D* mutants, R1–R6 project through the lamina, terminating in the medulla. Genetic mosaics, transgene rescue, and immunolocalization indicate PTP69D functions in R1–R6 growth cones. PTP69D overexpression in R7 and R8 does not respecify their connections, suggesting PTP69D acts in combination with other factors to determine target specificity. Structure–function analysis indicates the extracellular fibronectin type III domains and intracellular phosphatase activity are required for targeting. We propose PTP69D promotes R1–R6 targeting in response to extracellular signals by dephosphorylating substrate(s) in R1–R6 growth cones.

Introduction

The establishment of appropriate connections between neurons is essential for nervous system function. In many regions of the nervous system, neurons are arranged in layers and each layer is innervated by a distinct subset of axons (e.g., Bolz et al., 1996). Although substantial progress has been made toward understanding the molecular mechanisms underlying many aspects of axon guidance, the molecular logic by which layer-specific connections are established remains largely unknown (Tessier-Lavigne and Goodman, 1996). The visual system of *Drosophila melanogaster* provides a simple genetic system to address this question.

‖To whom correspondence should be addressed (e-mail: zipursky@hhmi.ucla.edu).
#These authors contributed equally to this work.

Different classes of photoreceptor neurons (R cells) in the *Drosophila* compound eye form layer-specific connections in the optic lobe. The eye contains some 800 ommatidia or facets, each containing eight R cells (R1–R8). Different subclasses of R cells project to different layers of the optic lobe. R1–R6 axons connect to targets in the lamina, while R7 and R8 axons project through this layer and form connections in a deeper layer, the medulla.

The formation of connections by R cells involves a complex dialog between R cell afferents and their targets in the developing optic lobe. R cell afferents induce the production and differentiation of lamina neurons as well as the migration and differentiation of lamina glia (Selleck and Steller, 1991; Winberg et al., 1992; Huang et al., 1998). The dependence of lamina differentiation on R cell–derived signals plays a crucial role in matching the number of afferents to their targets. R cell axons from each facet in the eye disc form a compact, highly ordered fascicle with the axons of R1–R7 surrounding the R8 axon (Meinertzhagen and Hanson, 1993). Axons from each bundle appear to enter the optic lobe in a sequential fashion: R8 enters first, followed by R1–R6, and then R7. Since target specificity does not simply reflect the order of axon ingrowth, target selection likely reflects molecular recognition between R cell axons and determinants in the developing optic lobe. Based on histological studies, Steller and colleagues proposed that initial targeting to the lamina is a consequence of interactions between R1–R6 growth cones and lamina glia (Perez and Steller, 1996). R1–R6 growth cones establish synaptic connections with lamina neurons during pupal development, some 4–5 days after projecting into the lamina. This involves a complex series of steps (Meinertzhagen and Hanson, 1993; T. Clandinin and S. L. Z., unpublished data), as R1–R6 growth cones undergo stereotyped rearrangements to establish their final pattern of connections. While inductive signals produced by R cells have been identified, the targeting signals in the optic lobe and their receptors on R cell growth cones remain unknown.

We previously described R1–R6 targeting errors in the *dreadlocks* (*dock*) mutant (Garrity et al., 1996). Since *dock* encodes an SH3/SH2 adapter protein, we pursued the possibility that phosphotyrosine signaling plays a crucial role in lamina targeting. A collection of mutations in genes that were previously implicated in growth cone function in the embryo and that encode proteins involved in phosphotyrosine signaling were examined for R1–R6 targeting defects (P. A. G. and S. L. Z., unpublished data). Mutations in the gene encoding the receptor tyrosine phosphatase PTP69D produced a striking defect.

PTP69D is one of three *Drosophila* receptor protein tyrosine phosphatases (RPTPs) known to play important roles in motor axon guidance (Desai et al., 1996, 1997; Krueger et al., 1996). These RPTPs have large extracellular domains containing multiple immunoglobulin (Ig) and/or fibronectin type III (FNIII) repeats, reminiscent of cell adhesion molecules (CAMs). Similar RPTPs are

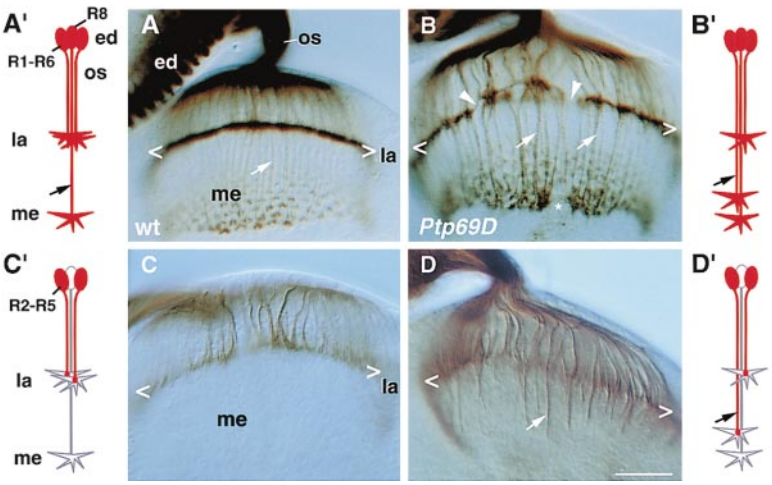

Figure 1. R1–R6 Neurons Project into the Medulla in *Ptp69D*

(A and B) Developing R cell projections in third instar larval eye–brain complexes visualized using mAb24B10. (A) In wild type, R cells in the developing eye disk (ed) project axons through the optic stalk (os) to targets in the developing optic lobes. R1–R6 axons stop in the lamina (la), forming a layer of expanded growth cones (the lamina plexus) (see Figure 4), while R7 and R8 growth cones terminate within the medulla (me) in a regular array.

(B) In *Ptp69D* mutants, the lamina plexus is discontinuous (arrowheads) and of variable thickness. Axon bundles projecting into the medulla are thicker than in wild type (arrows). This reflects the failure of many R1–R6 axons to terminate in the lamina target region (see [C] and [D]). The morphology and topographic organization of growth cones in the medulla are largely normal. A gap in the medulla pattern (asterisk) results from abnormal projection of Bolwig's nerve through this region during embryogenesis (C.-H. L. and S. L. Z., unpublished data).

(C and D) A subset of R1–R6 axons are visualized using the Ro-*lacZ*^{tau} marker (see text). In wild type (C), labeled axons terminate in the lamina (bracketed). In *Ptp69D* (D), labeled axons frequently terminate in the medulla.

(A′–D′) Schematic diagram of axonal projections from a single ommatidium (R1–R8 neurons) in wild-type (A′ and C′) and *Ptp69D* mutants (B′ and D′). (A′ and B′) mAb24B10 (red) marks both R1–R6 and R8 axons. (C′ and D′) The Ro-*lacZ*^{tau} marker labels a subset of R1–R6 axons (red). It does not stain the terminal expansion of these growth cones, since Tau localizes the marker protein to microtubules. Scale bar, 20 μm (A–D).

expressed on vertebrate growth cones (Stoker et al., 1995). The cytoplasmic tails of most RPTPs contain two tandemly arranged protein tyrosine phosphatase (PTP) catalytic domains. The membrane-proximal PTP domain (PTP1) provides most or all of the catalytic activity. The C-terminal PTP domain (PTP2) is proposed to play various regulatory roles such as mediating proper subcellular localization or serving as a binding site for downstream regulatory factors or substrates (Serra-Pages et al., 1995; Kashio et al., 1998; Wallace et al., 1998). The ligands and substrates involved in growth cone guidance by RPTPs are not known.

In this paper, we demonstrate that *Ptp69D* is necessary for R1–R6 axons to terminate in the lamina. In *Ptp69D* mutants, R1–R6 axons project through the lamina and terminate in the medulla. Genetic and biochemical studies support a model in which PTP69D functions in R1–R6 growth cones to detect an extracellular signal and translate it into changes in growth cone motility via the dephosphorylation of specific substrates. These studies provide an important step toward uncovering the molecular mechanisms underlying the specificity of neuronal connectivity in the fly visual system.

Results

PTP69D Is Required for R1–R6 Targeting

Ptp69D mutants were examined for R cell axon targeting defects by staining third instar larvae with the R cell–specific antibody mAb24B10 (Zipursky et al., 1984). In wild type (Figure 1A), R cell axon fascicles project through the optic stalk to appropriate topographic locations in the optic lobe. R1–R6 axons stop in the lamina, forming a dense layer of expanded growth cones, the lamina plexus, nestled between two layers of glial cells. R7 and R8 axons project through the lamina and terminate in the medulla, where they elaborate an array of expanded growth cones. In *Ptp69D* mutants (Figure 1B), R cell axons form a largely normal topographic array in both the lamina and medulla. However, the lamina plexus is wavy, of varying thickness, and discontinuous. In contrast to wild type, thicker than normal bundles of axons extend into the medulla. These features suggest that in *Ptp69D* mutants, many R1–R6 axons fail to stop in the lamina and terminate in the medulla.

R1–R6 axon mistargeting in *Ptp69D* was directly observed using a marker specific for a subset of R1–R6 axons, Ro-*lacZ*^{tau} (generously provided by U. Gaul). Ro-*lacZ*^{tau} encodes a Tau-β-galactosidase fusion protein (Callahan and Thomas, 1994) expressed under the control of the Rough enhancer, which is active largely in R2, R3, R4, and R5 (Heberlein and Rubin, 1990). In wild-type and *Ptp69D* heterozygotes, Ro-*lacZ*^{tau} predominantly labels axons that stop in the lamina (Figure 1C), as expected for an R2–R5-specific marker. In *Ptp69D* mutants, many LacZ-labeled axons do not stop in the lamina, terminating in the medulla (Figure 1D and Table 1). We estimate this represents mistargeting of 20%–25% of R2–R5 axon bundles (see Experimental Procedures). Many if not all mistargeted axons remain within the medulla in the adult (see below). Similar results were obtained using multiple heteroallelic combinations of *Ptp69D* (Desai et al., 1996). In summary, *Ptp69D* is required for targeting R1–R6 axons to the lamina.

PTP69D Functions in R Cells to Control R1–R6 Axon Targeting

A combination of genetic mosaic analysis and cell-specific transgene rescue experiments tested whether PTP69D was required in R cell afferents or their targets.

Table 1. Functional Analysis of PTP69D Mutants

	Transgene	LacZ-Labeled Axon Bundles in Medulla[a]	Targeting Rescue[b]
(A) Control			
Wild Type[c]	–	5 ± 3 (n = 17)	
69D mutant	–	29 ± 12 (n = 19)	
PTP69D-myc		8 ± 4 (n = 35)	+
(B) Extracellular Domain Mutants			
69DΔ(Ig)		7 ± 6 (n = 42)	+
69DΔ(FNIII)		23 ± 8 (n = 9)	–
69DΔ(Ig,FNIII)		22 ± 10 (n = 30)	–
69DΔ(FNIII,MPR)	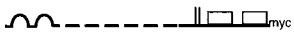	18 ± 5 (n = 36)	–
69DΔ(extra1)		n.d.[d]	–
(C) Intracellular Domain Mutants			
69D(DA1)		9 ± 4 (n = 21)	+
69D(DA1DA2)		21 ± 3 (n = 19)	–
69D(wedge)		6 ± 6 (n = 45)	+
69DΔ(PTP2)		7 ± 7 (n = 38)	+
(D) GMR-Driven Transgenes			
PTP69D		3 ± 2 (n = 10)	+
69D(DA1)	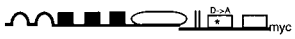	14 ± 3 (n = 13)	+
69D(DA1DA2)		26 ± 4 (n = 15)	–

Transgenes in (A–C) were driven in all neurons using Elav-*gal4.* Transgenes in (D) were driven in the eye using the GMR promoter. Rescue was assessed in a *Ptp69D*^{1}/*Df(3L)*^{8ex34} mutant background. A small fraction of labeled axons extends into the medulla in wild type. Using a specific marker to assess adult projections, however, no R2–R5 axons innervate the medulla (Figure 2). Thus, Ro-*lacZ*^{tau}-labeled axons observed in the wild-type larval medulla may reflect labeling of a few R8 axons, transient exploration of the medulla by R2–R5 axons, or disruptions in R2–R5 targeting caused by Tau binding to growth cone microtubules (Caceres and Kosik, 1990). Labeled axon bundles entering the medulla in wild type were thinner and appeared to contain fewer axons than in mutants; hence, the approximately 6-fold difference between wild type and mutant is likely an underestimate of the difference in the number of individual axons entering the medulla. However, this mutant transgene is expressed at very low levels (see text).

[a] Average number (± standard deviation) of labeled axon bundles extending into the medulla per hemisphere. n, total number of hemispheres examined.

[b] Targeting rescue: "+" denotes that the transgene rescued the *Ptp69D* phenotype as assessed by a significant decrease in the number of labeled axons in the medulla ($p < 0.0001$), while "–" indicates failure to rescue ($p > 0.0001$).

[c] "Wild type" indicates otherwise wild-type flies carrying one copy of Ro-*lacZ*^{tau} transgene.

[d] As judged by mAb24B10 staining, 69DΔ(extra1) fails to rescue *Ptp69D.*

In the genetic mosaic analysis, we examined targeting of *Ptp69D* mutant axons innervating normal (i.e., *Ptp69D*/+) brains. Mutant patches of retinal tissue were created by X-ray-induced mitotic recombination (see Experimental Procedures), and R1–R6 axon targeting was assessed in the adult using the R1–R6-specific marker Rh1-LacZ (Mismer and Rubin, 1987).

In wild-type and *Ptp69D* heterozygous adults, all R1–R6 axons terminated in the lamina (Figure 2A). In contrast, R1–R6 axons from all *Ptp69D* mutant eye patches analyzed (n = 11) projected through the lamina into the medulla (see below). To exclude the possibility that *Ptp69D* disrupts targeting indirectly by regulating cell fate and patterning in the eye, we examined plastic sections of homozygous mutant eye patches. Eye patterning, R cell fate determination, and cellular morphogenesis were largely normal in *Ptp69D* mutants (Figure 2D). Of 204 ommatidia scored from 21 eyes, only 3 ommatidia lacked a single R1–R6 neuron. Similar defects have been observed in other R cell axon guidance mutants and may reflect a weak requirement for normal innervation for R cell survival (Garrity et al., 1996; our unpublished data). Furthermore, as assessed by rhabdomere morphology, no transformations of R1–R6 neurons into R7 or R8 neurons were observed. Hence, targeting errors in *Ptp69D* do not result from more general defects in R cell development.

R1–R6 axons from small mutant patches exhibited R7- and R8-like axon trajectories into topographically appropriate positions in the medulla (Figure 2B). R1–R6 axons from larger mutant patches led to massive hyperinnervation of the medulla, disrupting its structure (Figure 2C). Thus, PTP69D is required in the eye for R1–R6 growth cones to terminate in the appropriate layer in the optic lobe. Furthermore, this defect is not corrected later in development, as R1–R6 axons persist in the medulla neuropil into the adult. The requirement of *Ptp69D* in the eye is underscored by the identification of *Ptp69D* alleles in a genetic screen for genes required in R cells for normal innervation of the optic lobe (T. Newsome, B. Åsling, and B. Dickson, personal communication).

To assess whether PTP69D was required only in the retina, and not in both the retina and optic lobe, we tested whether expressing PTP69D specifically in the retina rescued the targeting defect. A *Ptp69D* cDNA under the control of the eye-specific promoter GMR was introduced into a *Ptp69D* mutant background, and rescue was assessed in larvae using the Ro-*lacZ*^{tau} marker. Eye-specific expression of PTP69D fully rescued the R1–R6 axon targeting defect (Table 1). Since GMR drives expression in both neuronal and nonneuronal cells, it remained formally possible that PTP69D was required in nonneuronal retinal cells. However, expression of PTP69D via the neuron-specific Elav promoter rescued the R1–R6 axon targeting defect (Figure

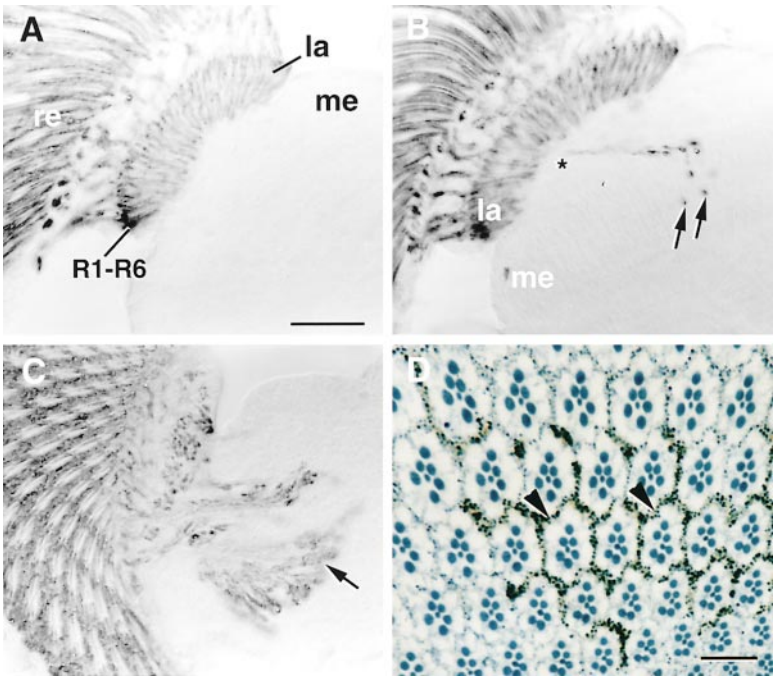

Figure 2. *Ptp69D* Is Required in the Eye

(A–C) R1–R6 axons were visualized using the R1–R6 marker Rh1-LacZ in adult head sections. (A) In wild type, all R1–R6 axons project from the retina (re) and terminate in the lamina (la); they do not extend into the medulla (me). (B) R1–R6 axons from a small patch of *Ptp69D* mutant tissue in the eye (pigment marker outlining mutant patch is not visible in this section due to antibody staining) project through the optic chiasm (asterisk) and into the medulla (arrows). (C) R1–R6 axons from a large patch innervating the medulla (arrow).

(D) *Ptp69D* mutant R cells differentiate normally as seen in toluidine blue–stained plastic sections. Since the mutant allele carries a dose-dependent *white* gene, the regions surrounded by dark pigment granules (arrowheads) contain homozygous $Ptp69D^{1}$ mutant R cells. Mutant ommatidia are indistinguishable from wild type. Scale bars, 20 μm (A–C) and 10 μm (D).

6A and Table 1), eliminating this possibility. Taken together, these results demonstrate that PTP69D functions in R cells.

R Cell Axons Induce Normal Lamina Development

The requirement of *Ptp69D* in R cell afferents is consistent with PTP69D detecting specific targeting signals in

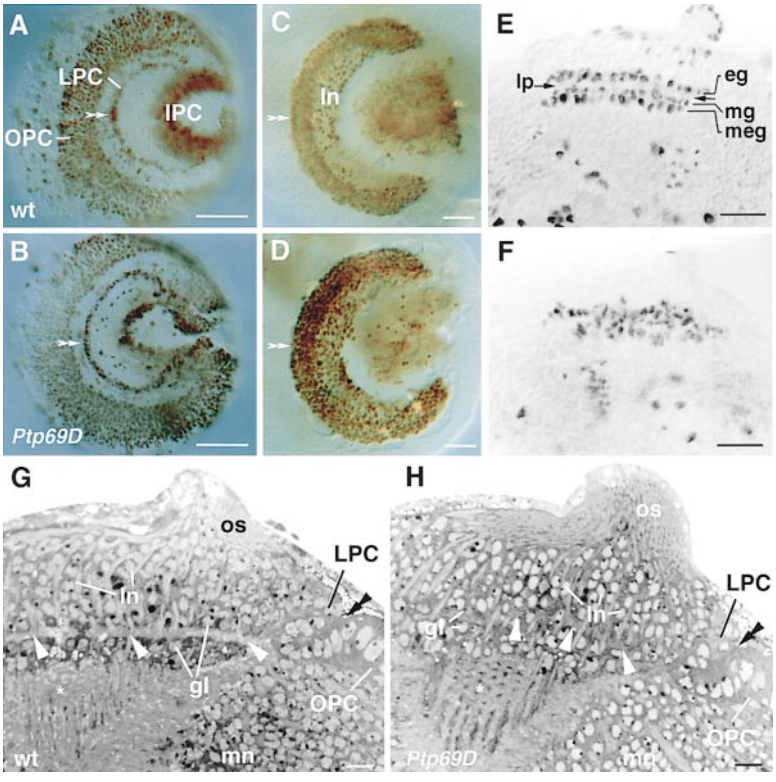

Figure 3. Target Development Is Normal in *Ptp69D*

(A and B) BrdU staining marks the three proliferation zones in the developing optic lobe: the outer proliferation center (OPC), the lamina precursor cells (LPC), and the inner proliferation center (IPC). Neuroblasts in the OPC give rise to the LPC. R cell afferents drive LPCs into S phase. Staining in wild type (A) and *Ptp69D* (B) is indistinguishable.

(C and D) Anti-Dachshund staining of lamina precursor cells posterior to the lamina furrow (double arrowheads) and lamina neurons (ln) is shown for wild type (C) and *Ptp69D* (D). Staining in *Ptp69D* is normal.

(E and F) Glial cells in cryostat section of third instar larval optic lobes were visualized with the anti-Repo antibody RK2, a glial-specific nuclear marker. In wild type, two rows of lamina glia, the epithelial (eg) and the marginal (mg) glia, are seen. The medulla glia (meg) lie medially to the marginal glia. R1–R6 growth cones terminate in the lamina plexus (lp, arrows). In *Ptp69D* (F), glial cells express the differentiation marker Repo. The layering of glial cells is disrupted.

(G and H) Plastic sections stained with toluidine blue reveal the structure of the optic lobe of wild type (G) and *Ptp69D* mutants (H). The shape and location of the OPC and the LPC in wild type and mutant are indistinguishable. Lamina neurons (ln) form columns in both mutant and wild type. In wild type, the lamina plexus (arrowheads) is seen as a lightly stained strip of tissue. In *Ptp69D*, it is discontinuous and of variable thickness. This correlates with the mistargeting of R1–R6 growth cones (see Figures 1B and 1D). Asterisk, medulla neuropil; double arrowhead, furrow separating LPC and OPC; gl, glial cells; mn, medulla neurons; os, optic stalk. Scale bars, 20 μm (A–H).

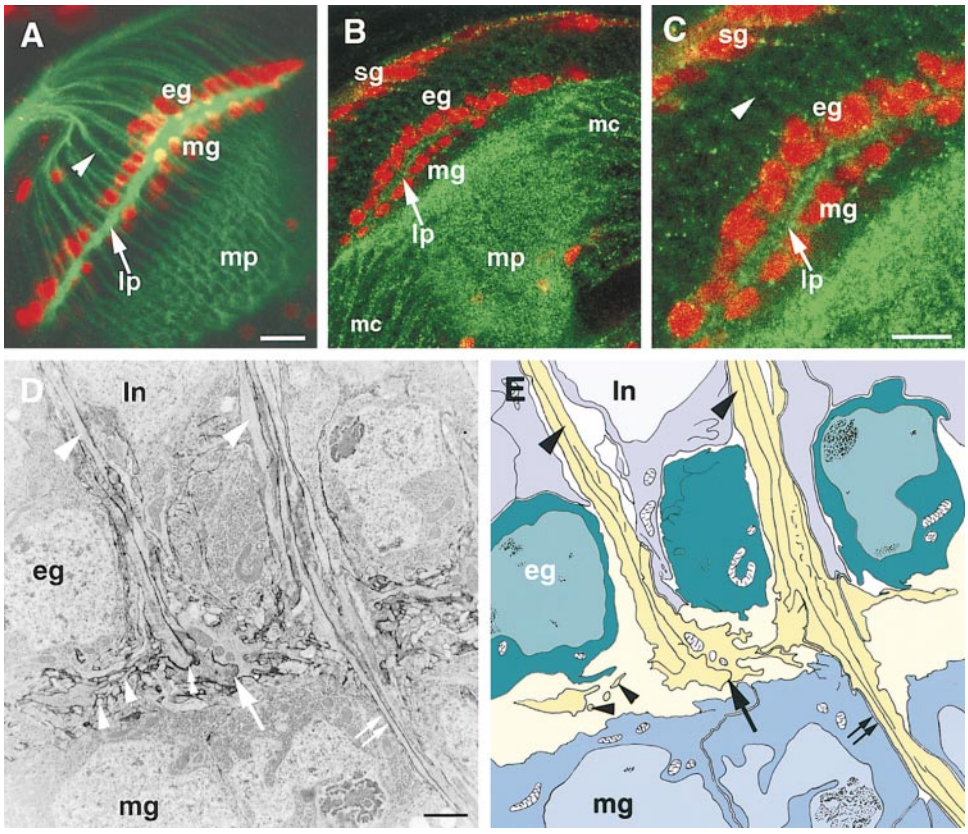

Figure 4. PTP69D Is Localized in the Lamina and Medulla Neuropils

Antibody-stained whole-mount preparations of larval eye–brain complexes were visualized using confocal laser microscopy.

(A) Photoreceptor axons (arrowhead) were labeled using mAb24B10 (green) and lamina glia using anti-LacZ staining (red) of the enhancer trap Gal4 line MZ1127 (Ito et al., 1995) driving the expression of nuclear LacZ. This glial line stains both the epithelial (eg) and marginal (mg) glia. The R1–R6 growth cones terminate in the lamina plexus (lp, arrow) between these two glial cell layers.

(B and C) PTP69D visualized with anti-PTP69D mAb 2C2 (green) is expressed in the lamina plexus and the medulla neuropil (mp). Glia were labeled with anti-LacZ using the glia-specific Gal4 line 1.3 D2 (S. Granderath and C. Klaembt, personal communication) driving nuclear LacZ. This marker stains epithelial, marginal, and satellite (sg) glia. Most if not all PTP69D immunoreactivity in the medulla can be attributed to expression in medulla neurons projecting into the neuropil from the adjacent medulla cortex (mc). (C) High magnification view of lamina plexus from (B).

(D and E) The lamina plexus in a wild-type third instar larvae visualized by electron microscopy. R cell growth cones were identified by the electron-dense DAB reaction product on their membranes (double arrowhead) using DiI labeling and subsequent photoconversion. A colorized tracing of (D) is shown in (E). Bundles of R cell axons project (large arrowheads) between columns of lamina neurons (ln). R1–R6 terminals stop between epithelial and marginal glial cells, and R7/R8 project through the marginal glia layer into the medulla neuropil. R1–R6 axons form groups of expanded growth cones (large arrow) within the lamina plexus (see bundle on left). These are surrounded by small diameter profiles of their filopodia (small arrowheads). In this sectioning plane, the axon bundle on the right can be followed through the lamina and between the marginal glia (small arrows). No synaptic contacts were observed at this stage of development. Scale bars, 20 μm (A and B), 10 μm (C), and 1 μm (D).

the lamina. Alternatively, PTP69D may be required in R cell growth cones to induce lamina target development and disrupt R1–R6 targeting only indirectly. To distinguish these possibilities, we assessed lamina development using specific markers and in plastic sections.

Two signals released from R cell growth cones act sequentially to induce lamina precursor cells (LPCs) to produce lamina neurons (Huang et al., 1998). Hedgehog drives G1-arrested LPCs into S phase of their final division. The epidermal growth factor receptor ligand Spitz then induces lamina neuron differentiation. In *Ptp69D* mutants, LPC proliferation and lamina neuron differentiation were normal, as assessed using anti-BrdU, anti-Dachshund (Figures 3A–3D), and anti-Elav staining (data not shown). The organization of lamina neurons into columns was also largely normal, as seen in semithin plastic sections (Figures 3G and 3H). Thus, *Ptp69D* is not required for lamina neuron induction.

R cell growth cones terminate between two rows of glial cells (see Figure 4). These cells depend on signals from R cell axons to migrate and to differentiate (Winberg et al., 1992; Perez and Steller, 1996). Glial differentiation was assessed using an antibody recognizing Repo, a glial-specific nuclear protein (Campbell et al., 1994). In *Ptp69D* (Figure 3F), as in wild type (Figure 3E), glia migrated into the lamina and expressed Repo. In contrast to wild type, however, they formed irregular rows. It seems most likely that disruption in glial layering is a consequence of the failure of R1–R6 growth cones to terminate in the lamina, giving rise to an uneven lamina

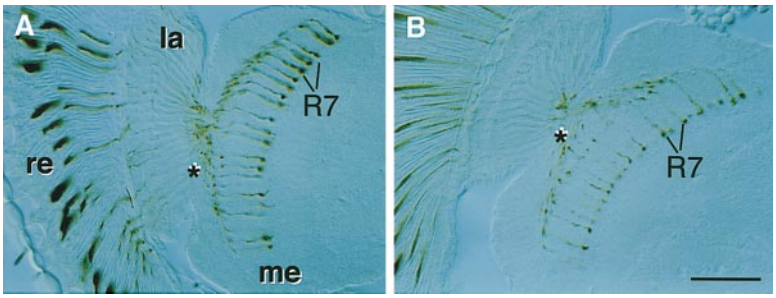

Figure 5. Expression of PTP69D in R Cells Is Not Sufficient to Retarget R7 Axons

(A and B) R7 projections were assessed using Rh4-LacZ (Fortini and Rubin, 1990), a marker expressed in a subset of R7 neurons, in cryostat sections stained with anti-LacZ antibody. In comparable sections of wild-type heads (A) and sections of heads carrying pGMR-PTP69D (i.e., driving high level of PTP69D expression in R cells) (B), similar numbers of R7 termini were observed in the medulla. la, lamina; me, medulla; re, retina; asterisk represents position of the first optic chiasm. Scale bar, 20 μm.

plexus of varying thickness separating glial layers. Thus, *Ptp69D* is probably not required for the differentiation of lamina glia.

PTP69D Protein Colocalizes with R1–R6 Growth Cones

Previous work demonstrated that PTP69D protein is present on R cell axons and in the optic lobe (Desai et al., 1994). To assess whether PTP69D could act as a receptor in R1–R6 growth cones to control targeting directly, we examined its distribution more precisely. Double-staining experiments using mAb24B10 and a nuclear glial marker show the dense layer of R cell growth cones between the epithelial and marginal glial cells (Figure 4A). Single-cell labeling experiments (P. A. G. et al., unpublished data) confirmed that R1–R6 growth cones terminate in this region. Electron microscopy revealed that at this stage in development, expanded R cell growth cones and their filopodia contribute the vast majority of processes to the lamina plexus and are in close juxtaposition to the epithelial and marginal glial cells (Figure 4D).

PTP69D protein distribution within the lamina was assessed in preparations double stained with both anti-PTP69D and a glial marker. Anti-PTP69D staining was observed in the lamina plexus between the epithelial and marginal glial cells (Figures 4B and 4C). Staining was observed at the anterior edge of the lamina plexus where newly arriving R1–R6 axons terminate. Thus, PTP69D protein colocalizes with R1–R6 growth cones in the lamina, indicating that it is expressed at the appropriate time and place to play a direct role in determining R1–R6 target specificity. PTP69D immunoreactivity was also detected in the medulla neuropil. Since medulla neurons projecting into this neuropil express PTP69D at very high levels, we were unable to determine whether the R7 and R8 axons in the medulla also have PTP69D on their surfaces.

PTP69D Is Not Sufficient to Retarget R7 and R8 Axons to the Lamina

We sought to test whether high levels of PTP69D were sufficient to retarget R7 and R8 growth cones to the lamina. The GMR promoter drives high-level expression in all R cells. This was not sufficient to retarget R8 axons to the lamina, as assessed with mAb24B10 larval staining (data not shown), nor to respecify R7 connections assessed in adults using an R7 axon–specific marker (Figure 5). Thus, PTP69D is necessary for R1–R6 axons to stop in the lamina, but it is not sufficient to promote retargeting of R7 and R8 axons (see Discussion).

Phosphatase Activity Is Essential for PTP69D Function

PTP69D has a CAM-like extracellular region and an intracellular region encoding two protein tyrosine phosphatase domains, PTP1 and PTP2. To determine which regions contribute to R1–R6 targeting, mutated *Ptp69D* cDNAs were assessed for their ability to rescue the *Ptp69D* R1–R6 targeting phenotype. Expression was driven either by the GMR promoter or *Elav-gal4* (Figure 6 and Table 1). All mutant constructs analyzed showed high levels of protein expression and axonal localization (data not shown). Multiple transgenic lines for each construct were tested. Rescue was quantified by counting Ro-*lacZ*^{tau}-labeled fascicles projecting into the medulla (Table 1).

The requirement for PTP catalytic activity was assessed by deletion analysis and by inactivating point mutations (Figures 6D–6F and Table 1). A construct lacking PTP2 [69DΔ(PTP2)] rescues R1–R6 axon targeting defects, demonstrating that this domain is dispensable for R1–R6 targeting. Unlike wild-type PTP69D, however, 69DΔ(PTP2) driven by *Elav-gal4* failed to restore viability beyond the pupal stage, indicating that PTP2 is required for other developmental processes.

To assess the role of phosphatase catalytic activity, a point mutation (D→A) was introduced into a conserved aspartate residue within the catalytic site of PTP1. Biochemical and structural studies in other receptor tyrosine phosphatases indicate that this conserved residue is important for phosphatase activity and that an alanine for aspartate substitution inhibits catalysis (see Discussion). Surprisingly, this mutant rescued the R1–R6 targeting phenotype. Thus, either phosphatase activity is not required, or PTP2 provides compensatory activity. To distinguish these models, the aspartate to alanine mutation was introduced into both PTP domains. This mutant does not rescue R1–R6 targeting. Thus, while the PTP1 domain is sufficient for rescue, both PTP1 and PTP2 can contribute to PTP69D function. These data indicate that PTP69D must dephosphorylate one or more substrates in R1–R6 growth cones to promote lamina targeting.

The FNIII Repeats Are Essential for PTP69D Function

The extracellular domain of PTP69D is composed of two Ig and three FNIII domains and a membrane-proximal

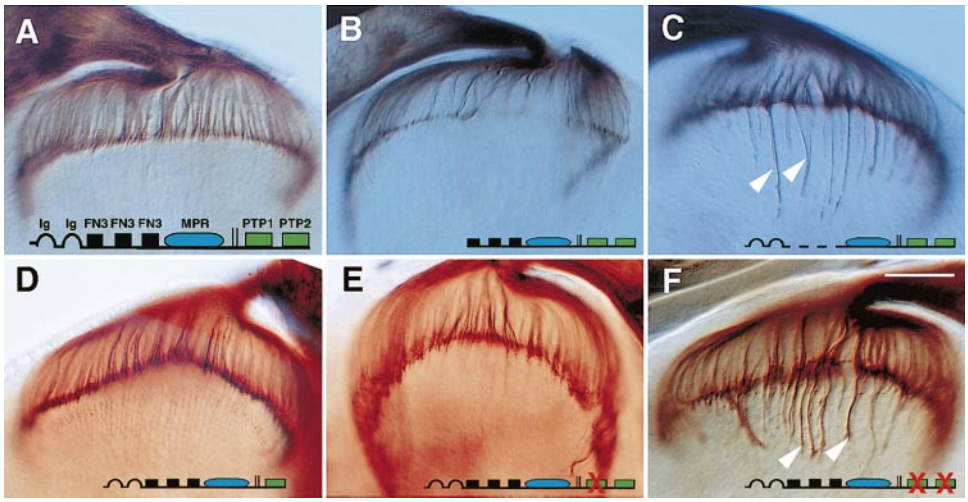

Figure 6. The FNIII Repeats and Tyrosine Phosphatase Activity Are Required for R1–R6 Targeting

The ability of various PTP69D mutants to restore *Ptp69D* targeting defects was assessed by expressing these constructs under UAS control using the panneuronal driver *Elav-gal4* in the *Ptp69D* mutant background. A subset of R1–R6 axons in whole-mount preparations of third instar larvae was visualized using Ro-*lacZ*^{tau} marker. For quantitation of rescue, see Table 1. For projection defects in *Ptp69D*, see Figure 1D. A schematic representation of the rescue constructs is shown at the bottom of each panel. Rescue of the *Ptp69D* mutant is seen with full-length PTP69D (A), 69DΔ(Ig) (B), 69DΔ(PTP2) (D), and 69D(DA1) (E). Rescue was not seen for 69DΔ(FNIII) (C) or for 69D(DA1DA2) (F). LacZ-labeled axons that extend into the medulla are indicated by arrowheads (see Experimental Procedures for details). Scale bar, 20 μm.

region (MPR) of some 300 amino acids with no detectable homology to other proteins. To determine which regions are critical for function, a series of deletion mutants were tested for their ability to rescue *Ptp69D* targeting defects (Table 1). Two mutant proteins containing essentially no extracellular domain (except for the signal sequence and 20 or 40 amino acids of the MPR) did not rescue *Ptp69D* R1–R6 targeting defects but were expressed at very low levels. Hence, the failure to rescue may reflect the level of expression rather than a requirement for the extracellular domain for PTP69D function.

Constructs lacking the Ig domains fully rescued the *Ptp69D* targeting phenotype (Figure 6B). While the Ig domains were not necessary for R1–R6 targeting, they were required to restore viability, indicating that they are important in other developmental contexts. Mutants lacking only the FNIII domains (Figure 6C), or larger deletions removing the Ig domains or the MPR in addition to the FNIII domain, did not rescue R1–R6 targeting or restore viability. Deletions removing only the MPR were not tested. In summary, these data support a model in which the FNIII domains bind targeting determinants in the lamina, translating them into changes in the catalytic activity, specificity, or localization of the tyrosine phosphatase domains.

PTP69D Is Proteolytically Cleaved

Previous studies demonstrated that a number of mammalian RPTPs (including LAR, RPTPμ, and RPTPσ) are cleaved within their extracellular domains (e.g., Streuli et al., 1992; Aicher et al., 1997). Since the extracellular domain can be shed from the cell surface, the extracellular and intracellular domains of these proteins may function separately. A model for PTP69D function in which ligand binding regulates the activity of the intracellular domain requires that the protein or a fraction thereof is not cleaved, or alternatively, if cleaved, the two fragments must remain associated. We therefore tested whether PTP69D was proteolytically cleaved and whether the extracellular and intracellular domains associate with each other (Figure 7).

A monoclonal antibody directed toward an N-terminal extracellular epitope of PTP69D recognized a single band of ~110 kDa on Western blots of extracts prepared from third instar eye–brain complexes (Figure 7C). Since this is substantially smaller than the size predicted based on its amino acid composition (about 180 kDa), it suggested that PTP69D could be proteolytically processed. This was examined further in S2 cell lines (Figure 7B) and in eye–brain complexes from transgenic animals expressing PTP69D (Figure 7C) with a C-terminal Myc-epitope tag. In transfected S2 cells, both the N- and C-terminal-directed antibodies recognized a common band of about 200 kDa, which we propose corresponds to the full-length glycosylated form of the protein. While the N-terminal-directed antibody recognized the 110 kDa species previously observed in extracts of eye–brain complexes, the C-terminal antibody recognized a band of about 90 kDa. Examination of the PTP69D sequence revealed a basic residue–rich sequence, KLRDKR, in the MPR (Figure 7A) that may serve as a proteolytic cleavage site to generate these two fragments (Streuli et al., 1992). Since the 200 kDa band was not observed in extracts of eye–brain complexes, proteolytic cleavage in the developing animal is efficient.

Since the PTP69D protein is cleaved, the ability of the two fragments to associate in transfected S2 cells was assessed. The C-terminal fragment of PTP69D was immunoprecipitated from S2 cells expressing the C-terminal epitope-tagged PTP69D using anti-Myc antibody. The N-terminal fragment was also found in the immunoprecipitate, indicating that some of the cleaved fragments remain associated with each other. Although

these results do not exclude a model in which the two fragments function separately, they are consistent with a model in which they function together in a complex to regulate targeting.

Discussion

In this paper, we demonstrate that a receptor tyrosine phosphatase, PTP69D, plays a crucial role in R1–R6 targeting. Targeting requires the FNIII domains and the tyrosine phosphatase activity. We propose that PTP69D, expressed on the surface of R1–R6 growth cones, detects specific signals in the developing lamina and translates them into a "stop" signal to the growth cone motility apparatus through the dephosphorylation of one or more substrates. The failure to terminate within the lamina leads to targeting of R1–R6 axons to an inappropriate layer in the optic lobe, the medulla. This is not a transient defect, as R1–R6 axons remain within the adult medulla neuropil.

PTP69D Regulates Lamina Targeting of R1–R6 Neurons

PTP69D is required for a specific step in a complex interplay between R cell afferents and cells in the lamina. Afferent growth cones produce a specific sequence of inductive signals, and different R cell afferents must distinguish between the target recognition signals in the lamina and medulla. PTP69D is required for R1–R6 neurons to terminate in the lamina, but it is not required to induce optic ganglion development. While the specific target recognition signals remain unknown, the intimate association of R1–R6 growth cones with the surface of the epithelial and marginal glia has led to the speculation that these cells provide such a signal (Perez and Steller, 1996). Alternatively, PTP69D may detect a signal from the medulla that repels R1–R6 growth cones from entering. Finally, PTP69D may promote R1–R6 targeting less directly. For instance, activation of a targeting receptor may lead to PTP69D-dependent inhibition of further extension along the R8 axon.

We estimate that in *Ptp69D* mutants, 20%–25% of the R1–R6 axon bundles extend beyond the lamina (see Experimental Procedures). Given that the *Ptp69D* alleles used are strong loss-of-function mutants (if not null), this level of expressivity is unlikely to reflect residual *Ptp69D* activity. Indeed, there is substantial precedent for strong loss-of-function mutations causing partial disruptions in axon guidance. For example, mutations in *C. elegans unc-6* (i.e., netrin) and its receptor *unc-40* disrupt the direction of outgrowth of only 35%–40% of the PDE neurons (Hedgecock et al., 1990). Incomplete mistargeting may reflect compensation by related receptor tyrosine phosphatases, the existence of redundant pathways regulating targeting, or that only a subpopulation of R1–R6 axons require *PTP69D*. Receptor tyrosine phosphatases have overlapping functions in embryonic motoneurons (Desai et al., 1997). Neither DPTP99A nor DLAR mutations lead to R1–R6 mistargeting (P. A. G. and S. L. Z., data not shown). Further studies analyzing double and triple mutant combinations will be necessary to critically assess redundancy between these RPTPs in the eye. As for the activity of parallel pathways acting in concert with *DPTP69D* to regulate R1–R6 target specificity, Goodman and colleagues have shown recently that motoneurons utilize a combination of multiple cues in determining target specificity in the developing fly embryo (Winberg et al., 1998). That multiple overlapping mechanisms regulate many aspects of guidance has emerged as a common

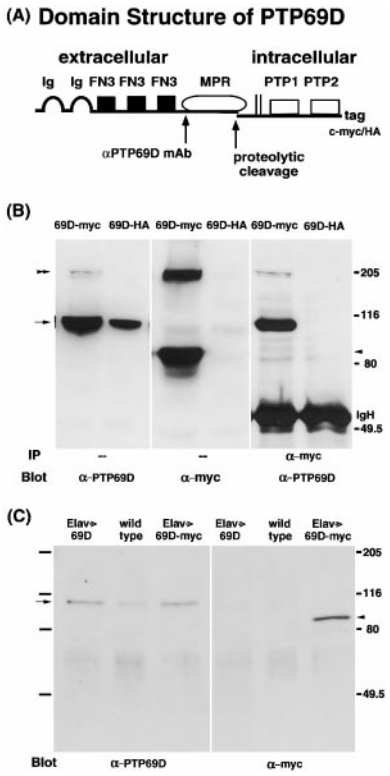

Figure 7. PTP69D Is Proteolytically Cleaved

(A) Schematic diagram of the domain structure of PTP69D based on primary sequence and biochemical data. The extracellular domain of PTP69D contains two Ig domains, three FNIII domains, and a membrane-proximal region of some 300 amino acids (MPR). The intracellular domain is composed of tandem phosphatase domains (PTP1 and PTP2). Proteolytic processing appears to occur within the MPR as judged from the relative sizes of the N- and C-terminal fragments. Anti-PTP69D is a mouse monoclonal antibody, 3F11, which recognizes an epitope in the N-terminal region of the MPR (C.-H. L., unpublished data). A Myc (or HA) tag was used to mark the C terminus. Western blots of protein preparation from transfected S2 cells (B) and third instar eye–brain complexes (C) probed with anti-PTP69D and anti-Myc monoclonal antibodies (as indicated below the blots) are shown.

(B) Extracts or immunoprecipitates of S2 cells transfected with either PTP69D-myc or PTP69D-HA were analyzed by Western blotting, as indicated. Unprocessed PTP69D (~200 kDa, double arrowhead) was detected with both N-terminal and C-terminal probes. Fragments of ~110 kDa (arrow) and ~90 kDa (arrowhead) were detected with the N- and C-terminal probes, respectively. The association between the N-terminal and C-terminal fragments was observed in Western blots of anti-Myc immunoprecipitates probed with anti-PTP69D antibody. Cells expressing HA-tagged PTP69D were used as a control for anti-Myc immunoprecipitation.

(C) Extracts were prepared from third instar eye–brain complexes in which PTP69D (or PTP69D-Myc) was driven specifically in neurons using the *gal4*/UAS system (i.e., *Elav-gal4*) and from wild type. Western blots were probed with anti-PTP69D or anti-Myc, as indicated. In the extracts, unprocessed PTP69D is not detected.

theme from studies in vertebrates and invertebrates (Tessier-Lavigne and Goodman, 1996).

High-level transgene expression of PTP69D in R7 and R8 growth cones was not sufficient to retarget them to the lamina. This may reflect inhibitory mechanisms in R7 and R8 that prevent lamina targeting and/or the existence of additional lamina determinants expressed in R1–R6 growth cones that act in a combinatorial fashion with PTP69D to determine layer specificity. Such determinants may include other surface recognition molecules or components of the signal transduction machinery in the growth cone.

The FNIII Region and Tyrosine Phosphatase Activity Are Required for Lamina Targeting

The extracellular CAM-like domain and intracellular phosphatase activity of PTP69D are critical for R1–R6 targeting. In both tissue culture and developing eye–brain complexes, PTP69D is cleaved into two parts, an N-terminal extracellular fragment and a C-terminal region containing the transmembrane segment and the intracellular domain. Immunoprecipitation experiments revealed that a fraction of these two fragments are associated. Although it remains possible that each fragment functions independently, our structure–function and biochemical results are consistent with these fragments acting together to control R1–R6 targeting.

While receptor tyrosine phosphatases play important developmental roles in flies, worms, and mammals (Chien, 1996; Kokel et al., 1998), little is known about their extracellular ligands and intracellular substrates. The best characterized receptor tyrosine phosphatase is CD45, which plays a crucial role in regulating signaling from both T and B cell receptors in the mammalian immune system (reviewed by Neel, 1997). CD45 promotes signaling by removing an inhibitory phosphate from Src family kinases in lymphocytes. Structure–function analysis of CD45 uncovered an essential role for the PTP1 domain for signaling. While the phosphatase activity of the PTP2 domain of CD45 is not required for its function, recent studies reveal a noncatalytic role for PTP2 (Kashio et al., 1998).

PTP1 of PTP69D is sufficient for R1–R6 targeting. While R1–R6 targeting is rescued by mutants deleted for PTP2, however, the failure to rescue *Ptp69D* mutants to viability underscores the function of PTP2 elsewhere in the organism. Surprisingly, a transgene [69D(DA1)] harboring a point mutation designed to disrupt PTP1 catalytic activity rescues the mutant phenotype. The aspartate to alanine (D→A) mutation produces a mutant protein that can act as a substrate trap (Flint et al., 1997): it can bind, but it does not efficiently hydrolyze, specific phosphotyrosine residues. As merely binding to targets may inhibit target protein function, D→A mutant proteins may retain residual biological function. Indeed, Simon and colleagues have shown that a catalytically inactive "substrate trap" mutant of the *Drosophila* Corkscrew phosphatase can rescue a weak loss-of-function *corkscrew* mutant (Allard et al., 1998). While residual biological activity may account for a portion of the 69D(DA1) rescue activity, the inability of a mutant transgene with both PTP1 and PTP2 D→A mutations [i.e., 69D(DA1DA2)] to rescue targeting revealed that PTP2 can also contribute appreciably to rescue. While the precise contribution of the PTP1 and PTP2 domains to R1–R6 targeting remain unresolved, these studies establish that tyrosine phosphatase activity is essential.

Structural studies of RPTPα and biochemical studies of an EGFR/CD45 chimera have led to the model that dimerization of RPTPs inhibits catalytic activity. In the crystal structure of RPTPα, the phosphatase domain forms a dimer with a segment of amino acids called "the wedge" of one monomer inserted into the catalytic cleft of its partner, thereby occluding the active site (Bilwes et al., 1996). Sequence alignment and modeling studies (data not shown) indicate that the PTP1 domain of PTP69D also contains a "wedge" structure. A mutation in the wedge region prevents dimerization-induced inactivation of the EGFR/CD45 chimera, providing support for the model of dimer-induced inhibition of phosphatase activity (Majeti et al., 1998). To assess whether this inhibitory mechanism plays a role in regulating PTP69D activity, the analogous mutation was made in the wedge region of PTP69D and the mutant transgene was introduced into flies. This mutant form fully rescued the targeting phenotype of the *Ptp69D* mutants (see Table 1). It showed poor rescue of lethality, however, suggesting that while this regulatory domain is dispensable for normal R1–R6 targeting, it plays an important role in other developmental contexts.

PTP69D Plays Multiple Roles in Axon Guidance

Mutations in *Ptp69D* cause different types of guidance defects in different neurons. For instance, while *Ptp69D* is necessary for R1–R6 neurons to stop in the lamina, it is required with other RPTPs for motoneuron growth cones within the intersegmental nerve to advance beyond specific landmarks toward their targets (Desai et al., 1997). Similarly, *Ptp69D* mutants exhibit diverse axon bundling defects. In double mutants of *Ptp69D* and the related RPTPs *Dlar* or *Ptp99A*, motor axons within the SNb fail to defasciculate upon entering their target region (Desai et al., 1997). Conversely, the normally fasciculated axons within Bolwig's nerve defasciculate in *Ptp69D* mutants (C.-H. L., D. Schmucker, and S. L. Z., unpublished data). That specific guidance molecules may function differently in different contexts is emerging as a common theme in neurodevelopment. Indeed, the netrin receptor (i.e., Dcc, Unc40) is required for both chemorepellent and chemoattractant function (Chan et al., 1996; Ming et al., 1997), as well as for fasciculation of specific axon bundles (D. Schmucker and S. L. Z., unpublished data). Hence, the same protein can subserve different functions in the context of different combinations of other guidance molecules. Combinatorial mechanisms provide the flexibility and complexity of interactions needed to establish large networks of connections between neurons with a limited number of signaling components. Future progress in dissecting the role of PTP69D in R1–R6 targeting will require identification of extracellular ligands and phosphatase substrates.

As in the fly visual system, the projection of neurons to specific layers of the brain is a prominent feature of neuronal organization in vertebrates. Studies in the cerebral cortex and the optic tectum argue for the importance of molecular targeting cues in establishing layer-specific connections (Bolz et al., 1996; Inoue and Sanes,

1997). As in flies, CAM-like RPTPs are expressed on axons and growth cones in the developing vertebrate CNS (e.g., Stoker et al., 1995). Given the conservation in function of other developmentally important molecules, it is tempting to speculate that CAM-like RPTPs will play a role in regulating layer specificity in the vertebrate brain.

Experimental Procedures

Genetics and Transformation

Ptp69D alleles are as described in Desai et al. (1996). Transformation was performed as in Rubin and Spradling (1982) and genetic mosaic analysis as in Garrity et al. (1996). For wild-type *Ptp69D* cDNA rescue with an eye-specific promoter, GMR-*Ptp69D*/+; *Ptp69D*^{1}/TM6b *Tb Hu* males were crossed to Df(3L)8ex34/TM6b *Tb Hu* females. For wild-type *Ptp69D* cDNA rescue using a neuron-specific driver, UAS-*Ptp69D*/+; *Ptp69D*^{1}/TM6b *Tb Hu* males were crossed to *Elav-gal4*, Df(3L)8ex34/TM6b *Tb Hu* females. *Tb*$^{+}$ flies were dissected and stained with mAb24B10 using HRP/DAB visualization to assess R cell axon projections. Anti-PTP69D mAb2C2 was subsequently visualized using a fluorescent secondary antibody to confirm the genotype and to determine whether the *Ptp69D* transgene was expressed. For genetic mosaic analysis, *Ptp69D*^{1} was used. X-ray-induced mitotic recombination generated mutant clones. Since the mutant chromosome carried a P[mini w^{+}] insert, homozygous mutant patches were dark red. The mutant chromosome also carries an additional lethal mutation. For rescue using *Ptp69D* mutant transgenes, males carrying UAS-*Ptp69D* or GMR-*Ptp69D* mutant transgenes in a Df(3L)8ex34/TM6b *Tb Hu* background were crossed to Ro-*lacZ*^{tau}, *Elav-gal4*, *Ptp69D*^{1}/TM6b *Tb Hu* females. Rescue was assessed by staining *Tb*$^{+}$ larvae with mouse anti-LacZ antibody and mAb2C2. Possible retargeting of R7 axons was assessed by crossing GMR-*Ptp69D*/Y males to Rh4-*lacZ* females and staining progeny with rabbit anti-LacZ antibody. Female and male progeny were the experimental and matched control samples, respectively.

Histology

For immunolabeling of whole-mount preparations and cryostat sections, as well as labeling of S phase cells, see Garrity et al. (1996). For confocal laser scanning microscopy (Bio-Rad), preparations were incubated with goat anti-rabbit or mouse IgG coupled to Cy3 or FITC, respectively (Jackson Immunoresearch). The preparation of toluidine blue–stained semithin sections of larval eye–brain complexes and adult heads for light microscopy, as well as DiI staining of photoreceptor neurons, subsequent photoconversion, and the preparation of ultrathin sections for electron microscopy (Zeiss EM 10) were essentially as described in Salecker and Boeckh (1995). Details of all protocols are available upon request.

Estimate of Mistargeting Expressivity

Approximately 20%–25% of R2–R5 axon bundles grow beyond the lamina in *Ptp69D* mutants. This estimate was obtained by dividing the mistargeted R2–R5 axon bundles (average number = 24) by the number of R2–R5 axon bundles contacting the lamina (between 90 and 115 bundles). The number of mistargeted bundles was calculated by subtracting the background level of Ro-*lacZ*^{tau}-labeled bundles entering the medulla in wild type (average number = 5) from the number observed in *Ptp69D* mutants (average number = 29). The total number of R2–R5 bundles contacting the lamina was calculated by estimating the number of ommatidia sending R2–R5 axons into the brain at the time point examined. *Ptp69D* mutant eye disks examined contained an average of 19 rows of developing ommatidia. R2–R5 development initiates some four rows behind the morphogenetic furrow, and these axons do not reach the brain until approximately four to five more rows of R2–R5 cells have developed (S. Kunes, personal communication). Thus, the average *Ptp69D* mutant brain examined was contacted by 10 to 11 rows of R2–R5 axons or 90 to 115 bundles.

Molecular Biology

pGMR-*Ptp69D* was constructed by subcloning the *Ptp69D* cDNA into the pGMR vector. To generate *Ptp69D* mutants, the *Ptp69D* cDNA was first amplified by PCR to introduce a BglII site at the 3′ end and then ligated to a vector containing a tandem Myc epitope (H. Hing and S. L. Z., unpublished). The resulting plasmid, 69D-*myc*/pBS, containing the *Ptp69D* cDNA with a C-terminal Myc tag, was used for subsequent mutagenesis. Deletion and point mutageneses were performed using the transformer site-directed mutagenesis kit (Clontech). Modified *Ptp69D* cDNAs were subcloned into pUAST or pGMR. The following PTP69D mutants were made: 69DΔ(Ig) encodes PTP69D with a deletion of the two Ig domains (residues 30–225); 69DΔ(FNIII) deletes the three FNIII domains (residues 236–534); 69DΔ(Ig, FNIII) deletes the Ig and the FNIII domains (residues 30–534); 69DΔ(FNIII, MPR) deletes the FNIII domains and the MPR (residues 236–796); 69DΔ(extra1) deletes the entire extracellular region (residues 30–796); 69DΔ(PTP2) deletes the second phosphatase domain (residues 1174–1462); 69D(DA1) has a point mutation in the catalytic aspartate residue (aspartate→alanine at residue 1065) in the first phosphatase domain; 69D(DA1DA2) has point mutations in the catalytic aspartate residues of the first and second phosphatase domains (aspartate→alanine at residues 1065 and 1354); 69D(wedge) has a point mutation in the wedge region of the first phosphatase domain (aspartate→arginine at residue 888). Detailed cloning procedures are available upon request.

Biochemistry

For expressing PTP69D in S2 cells, pUAS-*Ptp69D* or pUAS-*Ptp69D-myc* (described above) was cotransfected with pCoHygro (Invitrogen, for hygromycin resistance) and Gal4/pRmHa3, which contains the yeast transcription factor Gal4 under the control of metallothionine promoter (C.-H. L., unpublished data). Cell culture, transfection, and hygromycin selection to establish cell lines were performed according to the DES manual provided by Invitrogen. After the establishment of cell lines, $CuSO_4$ was added (0.5 μM) to induce Gal4, which in turn acted on the UAS promoter and induced the expression of PTP69D. The use of Gal4/pRmHa3 allows us to take advantage of the existing UAS constructs. We found the expression level is comparable to or higher than using the metallothionine promoter directly.

Cell lysis, immunoprecipitation, and immunoblotting were performed as described (Skolnik et al., 1991). Monoclonal anti-PTP69D antibody 3F11 has been described (Desai et al., 1994), and anti-Myc (9E10) and anti-HA antibodies were obtained from Santa Cruz and Babco, respectively.

Acknowledgments

We thank Ulrike Gaul for providing Ro-*lacZ*^{tau} flies and Christian Klaembt for gal4 line 1.3 D2 prior to publication. The authors thank the members of the Zipursky laboratory, Andreas Bergmann, Frank Gertler, Linda Huang, and Hermann Steller for comments on the manuscript and helpful discussion. P. A. G. has been supported by a Helen Hay Whitney Postdoctoral Fellowship, a Bank of America-Giannini Foundation Medical Research Fellowship, a Leukemia Society of America Special Fellowship, a McKnight Endowment Fund for Neuroscience Scholar Award, and startup funds from the Massachusetts Institute of Technology. C.-H. L. is a Howard Hughes Medical Institute Fellow of the Life Sciences Research Foundation. I. S. has been supported by a fellowship of Deutsche Forschungsgemeinschaft and by the Howard Hughes Medical Institute. K. Z. and C. J. D. were supported by NIH RO1 grant NS28182. S. L. Z. is an Investigator of the Howard Hughes Medical Institute. H. C. R. was supported by NIH predoctoral training grant 5 T32 GM07287-24.

Received January 25, 1999; revised February 26, 1999.

References

Aicher, B., Lerch, M.M., Muller, T., Schilling, J., and Ullrich, A. (1997). Cellular redistribution of protein tyrosine phosphatases LAR and PTPσ by inducible proteolytic processing. J. Cell Biol. *138*, 681–696.

Allard, J.D., Herbst, R., Carroll, P.M., and Simon, M.A. (1998). Mutational analysis of the SRC homology 2 domain protein-tyrosine phosphatase Corkscrew. J. Biol. Chem. *273*, 13129–13135.

Bilwes, A.M., den Hertog, J., Hunter, T., and Noel, J.P. (1996). Structural basis for inhibition of receptor protein-tyrosine phosphatase-α by dimerization. Nature *382*, 555–559.

Bolz, J., Castellani, V., Mann, F., and Henke-Fahle, S. (1996). Specification of layer-specific connections in the developing cortex. Prog. Brain Res. *108*, 41–54.

Callahan, C.A., and Thomas, J.B. (1994). Tau-β-galactosidase, an axon-targeted fusion protein. Proc. Natl. Acad. Sci. USA *91*, 5972–5976.

Campbell, G., Goring, H., Lin, T., Spana, E., Andersson, S., Doe, C.Q., and Tomlinson, A. (1994). RK2, a glial-specific homeodomain protein required for embryonic nerve cord condensation and viability in *Drosophila*. Development *120*, 2957–2966.

Chan, S.S., Zheng, H., Su, M.W., Wilk, R., Killeen, M.T., Hedgecock, E.M., and Culotti, J.G. (1996). UNC-40, a *C. elegans* homolog of DCC (Deleted in Colorectal Cancer), is required in motile cells responding to UNC-6 netrin cues. Cell *87*, 187–195.

Chien, C.B. (1996). PY in the fly: receptor-like tyrosine phosphatases in axonal pathfinding. Neuron *16*, 1065–1068.

Desai, C.J., Popova, E., and Zinn, K. (1994). A *Drosophila* receptor tyrosine phosphatase expressed in the embryonic CNS and larval optic lobes is a member of the set of proteins bearing the 'HRP' carbohydrate epitope. J. Neurosci. *14*, 7272–7283.

Desai, C.J., Gindhart, J.G., Jr., Goldstein, L.S.B., and Zinn, K. (1996). Receptor tyrosine phosphatases are required for motor axon guidance in the *Drosophila* embryo. Cell *84*, 599–609.

Desai, C.J., Krueger, N.X., Saito, H., and Zinn, K. (1997). Competition and cooperation among receptor tyrosine phosphatases control motoneuron growth cone guidance in *Drosophila*. Development *124*, 1941–1952.

Flint, A.J., Tiganis, T., Barford, D., and Tonks, N.K. (1997). Development of "substrate-trapping" mutants to identify physiological substrates of protein tyrosine phosphatases. Proc. Natl. Acad. Sci. USA *94*, 1680–1685.

Fortini, M.E., and Rubin, G.M. (1990). Analysis of cis-acting requirements of the Rh3 and Rh4 genes reveals a bipartite organization to rhodopsin promoters in *Drosophila melanogaster*. Genes Dev. *4*, 444–463.

Garrity, P.A., Rao, Y., Salecker, I., McGlade, J., Pawson, T., and Zipursky, S.L. (1996). *Drosophila* photoreceptor axon guidance and targeting requires the Dreadlocks SH2/SH3 adapter protein. Cell *85*, 639–650.

Heberlein, U., and Rubin, G.M. (1990). Structural and functional comparisons of the *Drosophila virilis* and *Drosophila melanogaster* rough genes. Proc. Natl. Acad. Sci. USA *87*, 5916–5920.

Hedgecock, E.M., Culotti, J.G., and Hall, D.H. (1990). The *unc-5*, *unc-6*, and *unc-40* genes guide circumferential migrations of pioneer axons and mesodermal cells on the epidermis in *C. elegans*. Neuron *2*, 61–85.

Huang, Z., Shilo, B.-Z., and Kunes, S. (1998). A retinal axon fascicle uses Spitz, an EGF receptor ligand, to construct a synaptic cartridge in the brain of *Drosophila*. Cell *95*, 693–703.

Inoue, A., and Sanes, J.R. (1997). Lamina-specific connectivity in the brain: regulation by N-cadherin, neurotrophins, and glycoconjugates. Science *276*, 1428–1431.

Ito, K., Urban, J., and Technau, G.M. (1995). Distribution, classification, and development of *Drosophila* glial cells in the late embryonic and early larval ventral cord. Roux's Arch. Dev. Biol. *204*, 284–307.

Kashio, N., Matsumoto, W., Parker, S., and Rothstein, D.M. (1998). The second domain of the CD45 protein tyrosine phosphatase is critical for interleukin-2 secretion and substrate recruitment of TCR-ζ in vivo. J. Biol. Chem. *273*, 33856–33863.

Kokel, M., Borland, C.Z., DeLong, L., Horvitz, H.R., and Stern, M.J. (1998). clr-1 encodes a receptor tyrosine phosphatase that negatively regulates an FGF receptor signaling pathway in *Caenorhabditis elegans*. Genes Dev. *12*, 1425–1437.

Krueger, N.X., Van Vactor, D.V., Wang, H., Gelbart, H., Goodman, C.S., and Saito, H. (1996). The transmembrane tyrosine phosphatase DLAR controls motor axon guidance in *Drosophila*. Cell *84*, 611–622.

Majeti, R., Bilwes, A.M., Noel, J.P., Hunter, T., and Weiss, A. (1998). Dimerization-induced inhibition of receptor protein tyrosine phosphatase function through an inhibitory wedge. Science *279*, 88–91.

Meinertzhagen, I.A., and Hanson, T.E. (1993). The development of the optic lobe. In The Development of *Drosophila melanogaster*, M. Bate and A. Martinez-Arias, eds. (Cold Spring Harbor, NY: Cold Spring Harbor Press), pp. 1363–1491.

Ming, G.L., Song, H.J., Berninger, B., Holt, C.E., Tessier-Lavigne, M., and Poo, M.-M. (1997). cAMP-dependent growth cone guidance by netrin-1. Neuron *19*, 1225–1235.

Mismer, D., and Rubin, G.M. (1987). Analysis of the promoter of the *ninaE* opsin gene in *Drosophila melanogaster*. Genetics *116*, 565–578.

Neel, B.G. (1997). Role of phosphatases in lymphocyte activation. Curr. Opin. Immunol. *9*, 405–420.

Perez, S.E., and Steller, H. (1996). Migration of glial cells into retinal axon target field in *Drosophila melanogaster*. J. Neurobiol. *30*, 359–373.

Rubin, G.M., and Spradling, A.C. (1982). Genetic transformation of *Drosophila* with transposable element vectors. Science *218*, 348–353.

Salecker, I., and Boeckh, J. (1995). Embryonic development of the antennal lobes of a hemimetabolous insect, the cockroach *Periplaneta americana*: light and electron microscopic observations. J. Comp. Neurol. *352*, 33–54.

Selleck, S.B., and Steller, H. (1991). The influence of retinal innervation on neurogenesis in the first optic ganglion of *Drosophila*. Neuron *6*, 83–99.

Serra-Pages, C., Kedersha, N.L., Fazikas, L., Medley, Q., Debant, A., and Streuli, M. (1995). The LAR transmembrane protein tyrosine phosphatase and a coiled-coil LAR-interacting protein co-localize at focal adhesions. EMBO J. *14*, 2827–2838.

Skolnik, E.Y., Margolis, B., Mohammadi, M., Lowenstein, E., Fischer, R., Drepps, A., Ullrich, A., and Schlessinger, J. (1991). Cloning of PI3 kinase–associated p85 utilizing a novel method for expression/cloning of target proteins for receptor tyrosine kinases. Cell *65*, 83–90.

Stoker, A.W., Gehrig, B., Haj, F., and Bay, B.H. (1995). Axonal localisation of the CAM-like tyrosine phosphatase CRYPα: a signaling molecule of embryonic growth cones. Development *121*, 1833–1844.

Streuli, M., Krueger, N.X., Ariniello, P.D., Tang, M., Munro, J.M., Blattler, W.A., Adler, D.A., Disteche, C.M., and Saito, H. (1992). Expression of the receptor-linked protein tyrosine phosphatase LAR: proteolytic cleavage and shedding of the CAM-like extracellular region. EMBO J. *11*, 897–907.

Tessier-Lavigne, M., and Goodman, C.S. (1996). The molecular biology of axon guidance. Science *274*, 1123–1133.

Wallace, M.J., Fladd, C., Batt, J., and Rotin, D. (1998). The second catalytic domain of protein tyrosine phosphatase δ (PTPδ) binds to and inhibits the first catalytic domain of PTPσ. Mol. Cell. Biol. *18*, 2608–2616.

Winberg, M.L., Perez, S.E., and Steller, H. (1992). Generation and early differentiation of glial cells in the first optic ganglion of *Drosophila melanogaster*. Development *115*, 903–911.

Winberg, M.L., Mitchell, K.J., and Goodman, C.S. (1998). Genetic analysis of the mechanisms controlling target selection: complementary and combinatorial functions of netrins, semaphorins, and IgCAMs. Cell *93*, 581–591.

Zipursky, S.L., Venkatesh, T.R., Teplow, D.B., and Benzer, S. (1984). Neuronal development in the *Drosophila* retina: monoclonal antibodies as molecular probes. Cell *36*, 15–26.